

THE FeII OPTICAL EMISSION IN AGN

C. BONGARDO, R. ZAMANOV, P. MARZIANI, M. CALVANI

INAF, Osservatorio Astronomico di Padova, Italy

J.W. SULENTIC

*Department of Physics and Astronomy, University of Alabama at
Tuscaloosa, USA*

We investigated the FeII optical emission in a sample of about 220 low-redshift quasars and luminous Seyfert 1 galaxies. We found that a scaled and broadened FeII template based on the I Zw 1 spectrum satisfactorily reproduce the FeII emission of almost all AGN of our sample. We also confirm that FWHM of $H\beta$ and $\text{FeII}\lambda 4570$ are tightly correlated. However, the correlation takes two slightly different forms: (a) if $\text{FWHM}(H\beta) \leq 4000 \text{ km s}^{-1}$ (Population A), the width of FeII and $H\beta$ is statistically indistinguishable, while the $\text{FWHM}(\text{FeII}\lambda 4570)$ is systematically lower than that of $H\beta$ if $\text{FWHM}(H\beta) \geq 4000 \text{ km s}^{-1}$ (Population B). This suggests that FeII emission in Pop. B sources may come from the outer part of $H\beta$ emitting region, where the ionization degree is lower.

1 Introduction

FeII emission has not been fully exploited as a diagnostic, because the complexity of the Fe^+ atom hampers reliable modeling. It was long ago realized that the FeII is emitted in the BLR. Strong FeII emission requires high density ($n_e \geq 10^9 \text{ cm}^{-3}$, high column density and low temperature ($T_e \approx 5000 \text{ K}$; [1]). These conditions are thought to be met in a partially ionized region within the BLR created by the strong X-ray emission in AGN ([2], [3] and [4]). The main observational evidence for BLR FeII emission is the profile FWHM similarity between $\text{FeII}\lambda 4570$ and the Broad Component of $H\beta$ ([5] and [6]). We show that an $\text{FWHM}(\text{FeII}\lambda 4570)$ vs. $\text{FWHM}(H\beta)$ correlation is highly significant for a large sample of AGN, but takes a different form depending on $\text{FWHM}(H\beta)$ and FeII intensity.

2 The Template

We analyzed 220 spectra of low- z quasars and luminous Seyfert 1 covering the $H\beta$ spectral range. For each spectrum, we measured the FeII emission using a scaled and broadened template extracted from a high S/N spectrum of I Zw

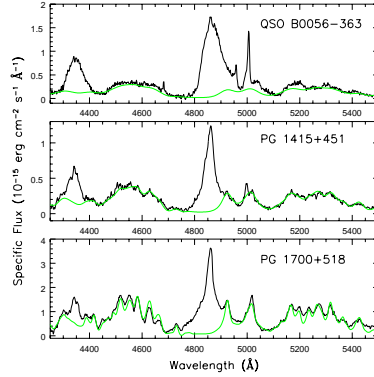


Figure 1: The $H\beta$ region, with the FeII_{opt} emission superimposed (thick green line).

1. This method has been already successfully applied by [7] and [8]. The template allows us to satisfactorily subtract the FeII emission to about 98% of the spectra of our sample. In other words, we found very few cases in which the line and multiplet FeII ratios deviate from the ones of I Zw 1. Fig. 1 shows the successful rendering of the FeII_{opt} emission by our template for three objects with very different line width.

3 FWHM($\text{FeII}\lambda 4570$) vs. FWHM($H\beta$)

Measurements of the FeII width are not trivial. To obtain a reliable estimate of the FWHM of FeII_{opt} lines we performed the following operations. (1) We defined the local continuum using the regions around 4200, 4700 and 5000 Å, which are relatively uncontaminated by FeII emission. (2) We subtracted our FeII template, scaled and broadened to obtain minimum residuals in correspondence of the FeII blend centered at 4570 Å. (3) At this point, we measured the broadening factor of the template, which is proportional to the FWHM($\text{FeII}\lambda 4570$), since the line FWHM is much larger than the instrumental profile. (4) We usually estimated the FWHM uncertainty evaluating a matrix where residuals were shown as a function of FeII intensity and broadening factor; FWHM boundaries were set when residuals were significantly worse than for the best fit. FeII equivalent width and FWHM measurements reliability depends on S/N ratio and intrinsic width of emission. For a fixed S/N, there is a minimum $W(\text{FeII})$ for which the blends become undetectable (i.e., features are lost in noise or create a pseudo-continuum). FeII equivalent width measurements were obtained for 112 objects; for the remaining only an upper limit to $W(\text{FeII})$ was given. The FWHM was measured for most but not all of the 112 objects: especially when FeII_{opt} emission was weak, it was not always

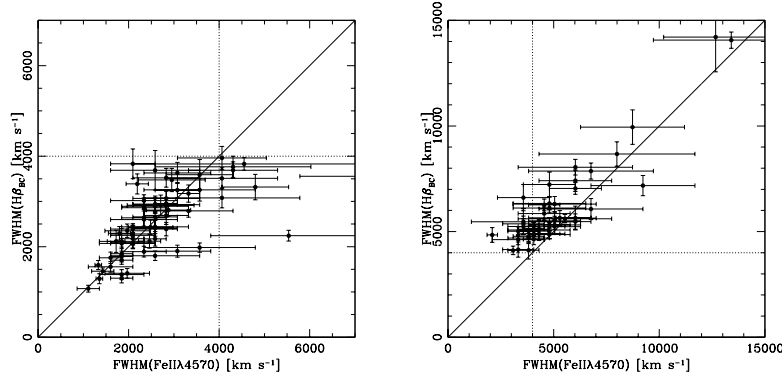


Figure 2: Comparison between $\text{FWHM}(\text{H}\beta_{BC})$ and $\text{FWHM}(\text{FeII}\lambda 4570)$ for AGN of Pop. A (left) and Pop. B (right).

possible to constrain its width.

To accurately measure $\text{FWHM}(\text{H}\beta_{BC})$ we further subtracted the $[\text{OIII}]$ emission at $\lambda 4959$ and $\lambda 5007 \text{ \AA}$, interpolating between the blue and the red edges of the lines. Whenever the broad and/or narrow components of $\text{HeII}\lambda 4686$ were visible, they were subtracted using a Gaussian fit. Last, we subtracted the narrow component of $\text{H}\beta$ also using a Gaussian profile.

Fig. 2 shows $\text{FWHM}(\text{FeII}\lambda 4570)$ vs. $\text{FWHM}(\text{H}\beta)$. There is a very well-defined correlation. Outlying data points are most likely due to poor S/N ratio, resolution and FeII weakness rather than to real differences. One case only is convincing: IRAS 07598+6508 (see §3.1).

The correlation takes a different form if $\text{FWHM}(\text{H}\beta) \leq 4000 \text{ km s}^{-1}$ (Population A, according to [9]) or $\text{FWHM}(\text{H}\beta) \geq 4000 \text{ km s}^{-1}$ (Population B):

- Pop. A. There is a tight correlation ($R_{\text{Pearson}} = 0.693$, $N = 69$, $P = 8.5 \times 10^{-9}$), with $\text{FWHM}(\text{H}\beta) \approx \text{FWHM}(\text{FeII}\lambda 4570)$. This implies that both emissions came from the same emitting region.
- Pop. B. Also in this case there is a clear correlation ($R_{\text{Pearson}} = 0.882$, $N = 43$, $P = 7.3 \times 10^{-9}$), but $\text{FWHM}(\text{H}\beta_{BC})$ seem to systematically exceed $\text{FWHM}(\text{FeII}\lambda 4570)$.

3.1 A special case: IRAS 07598+6508

This intriguing object shows a FIR excess and its location in the so-called optical Eigenvector 1 diagram is peculiar ([10]). It is interesting to note that

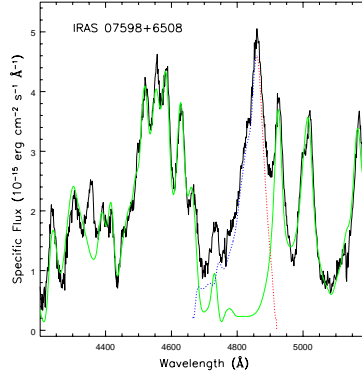


Figure 3: $H\beta$ region of IRAS 07598+6508. The dotted blue/red line represents the $H\beta_{BC}$.

$\text{FWHM}(H\beta_{BC})=5000\pm400 \text{ km s}^{-1}$ and $\text{FWHM}(\text{FeII}\lambda4570)=2000\pm1300 \text{ km s}^{-1}$. The good S/N ratio and the strength of the FeII_{opt} emission, along with the large $\text{EW}(H\beta_{BC})$, make this result especially striking. The strong blueward asymmetry of the BC of $H\beta$ (see fig. 3) suggests that an additional broadening may be due to Balmer emission associated to the highly blueshifted $\text{CIV}\lambda1549 \text{ \AA}$ emission). A narrower, unshifted component is to be associated to low ionization emission as in the rest of AGN.

4 Conclusion

The most straightforward implications of our results are that the FeII_{opt} emission mechanism is probably the same in almost all AGN, and that FeII_{opt} is emitted mainly from the zone of the BLR where $H\beta$ is also emitted. The FWHM of FeII_{opt} in Population B objects seems to be systematically narrower than that of the $H\beta$. This suggests that FeII emission in Pop. B sources may come from the outer part of $H\beta$ emitting region, where the ionization degree is lower.

Acknowledgements

We acknowledge financial support from the Italian MURST through Cofin 00-02-004.

References

1. S. Collin-Souffrin, M. Joly, S. Dumont, N. Heidmann, *A&A* **83**, 190 (1980).
2. J. Kwan and J.H. Krolik, *ApJ* **250**, 478 (1981).
3. J.H. Krolik and T.R. Kallaman, *ApJ* **324**, 714 (1988).

4. S. Collin-Souffrin, J.P. Lasota, *PASP* **100**, 1041 (1988).
5. M.M. Phillips, *ApJ* **226**, 736 (1978a).
6. M.M. Phillips, *ApJ* **38**, 187 (1978b).
7. T.A. Boroson and R.F. Green, *ApJS*. **80**, 109 (1992).
8. P.Marziani, J.W. Sulentic, D. Dultzin-Hacyan, M. Calvani, M. Moles *ApJS*. **104**, 37 (1996).
9. J.W. Sulentic, P.Marziani, D. Dultzin-Hacyan *ARA&A* **38**, 521 (2000).
10. P. Marziani, J.W. Sulentic, T. Zwitter, D. Dultzin-Hacyan, M. Calvani *ApJ* **558**, 553 (2001).